

JOM 23381

Study of CoGa deposition from the single source precursor $(\text{CO})_4\text{CoGaCl}_2(\text{THF})$

F. Maury *, L. Brandt and H.D. Kaesz

Department of Chemistry and Biochemistry, University of California, Los Angeles, CA 90024-1569 (USA)

(Received June 18, 1992)

Abstract

Depositions of thin films of CoGa from the single-source precursor $(\text{CO})_4\text{CoGaCl}_2(\text{THF})$ (**1**) have been carried out in an epitaxial organometallic chemical vapor deposition reactor. Prior to deposition, mass spectrometric (MS) and thermogravimetric (TGA) analyses of **1** were undertaken. Electron impact MS reveals a tendency for **1** partially to disproportionate (after loss of THF) into $\text{ClGa}(\text{CoCO})_4$ and GaCl_3 at probe temperature (120°C). The parent molecular ion for **1** appears with only low relative intensity (1%) indicating easy loss of THF as the first step. The principal features of the spectrum can be assigned to step-wise CO-loss series of peaks derived from three parent ions $[(\text{CO})_4\text{CoGaCl}_2]^+$ (a), $[(\text{CO})_4\text{CoGaCl}]^+$ (b), and $[(\text{CO})_4\text{Co}]^+$ (c). The relatively high intensity of the peaks derived from parent ions (a) and (b) indicate a relatively good stability of the Co–Ga bond through to the species $[\text{CoGa}]^+$ (rel. int. 15%). TGA of **1** under Ar shows decomposition in a single step in the range 100 to 230°C; residual weight of 44% is higher than expected for CoGa alone. Under H_2 however, a multistep decomposition process is observed culminating at 400–450°C; residual weight is 33%, close to that expected for CoGa.

In the (cold wall) CVD reactor, optimum deposition occurs under reduced pressure (0.9–6 torr) and laminar flow conditions using H_2 as carrier gas for (100)GaAs, (100)Si, and Al_2O_3 as substrates; growth rates are about 1.8 $\mu\text{m}/\text{h}$. Polycrystalline films are obtained under all conditions; annealing under H_2 for 2 h at 500°C gives relatively sharp XRD patterns for β -CoGa. For depositions in the range 250 to 350°C the Co/Ga ratio in the films is close to 1/1 showing control of stoichiometry by the precursor. These films however still contain some Cl. In the range 350 to 400°C the Cl content is lowered, however, the films become Co rich indicating loss of Cl is accompanied by loss of Ga. The stoichiometric control achieved in the present work indicates that single source precursors of ratio CoGa_2 could give Ga rich (64 at.% Ga) β -cubic CoGa for lattice matching to (100)GaAs.

1. Introduction

The evolving need for thin films of binary compounds offers an opportunity for the use of specially tailored organometallic compounds for chemical vapor deposition (OMCVD). A growing effort has been made on the design and synthesis of single source precursors for the deposition of III–V semiconductor compounds [1–3]. The advantages and drawbacks of organometallic single source precursors to control the stoichiometry of the films have been discussed in recent reviews [2,3].

This approach has also been investigated for the preparation of various other materials including, for instance, metal oxides [4], borides [5], silicides [6] and pnictides [7]. Heteronuclear carbonyl clusters have been used in attempts to deposit metal alloys [8].

Previously, we have reported the polycrystalline growth of CoGa and PtGa₂ thin films by OMCVD using the single source precursors $(\text{CO})_4\text{CoGaCl}_2(\text{THF})$ (**1**) and $\text{Pt}\{(\text{N}_2\text{C}_2(\text{CH}_3)_2\text{O}_2)(\text{GaMe}_2)\}_2$ (**2**), respectively [9]. Thin films of PtGa have been obtained [10a] from the precursor $[\text{cis}-(\text{Cy}_2\text{PCH}_2\text{CH}_2\text{PCy}_2)(\text{neo-Pe})\text{PtGa}(\text{neo-Pe})_2]$ (Cy = *c*-C₆H₁₁; neo-Pe = CH₂C(CH₃)₃) [10b]. This is noteworthy in light of the rather complicated Pt/Ga phase diagram which contains at least *nine* stable phases between pure Ga and pure Pt [10c]. Thus through OMCVD a degree of control of stoichiometry is possible that is not achieved in direct

Correspondence to: Prof. H.D. Kaesz or Dr. F. Maury.

* Permanent address: CNRS-URA 445, Ecole Nationale Supérieure de Chimie, 118, route de Narbonne, 31077 Toulouse Cedex (France).

evaporation methods such as molecular beam epitaxy (MBE).

Transition metal gallides and aluminides are attractive intermetallic compounds because they can grow epitaxially on III–V semiconductor compounds to form thermodynamically stable metal/semiconductor interfaces. Such heterostructures are usually constructed by MBE [11] but recently, we have demonstrated the epitaxial growth of CoGa on GaAs by OMCVD using the separate sources $(\eta^5\text{-C}_5\text{H}_5)_2\text{Co}(\text{CO})_2$ (3) and Et_3Ga (4) [12,13]. In the present study we describe a complementary study of the behavior of compound 1 as a single source precursor for the epitaxial growth of CoGa layers.

2. Experimental details

2.1. Synthesis and physico-chemical features of $(\text{CO})_4\text{CoGaCl}_2(\text{THF})$ (1)

This compound has been synthesized from $\text{Co}_2(\text{CO})_8$ and Ga_2Cl_4 according to the procedure reported in the literature [14]; the starting materials were purchased from Strem Chemicals Inc. (Newburyport, MA). After purification by re-crystallization in n-hexane, a white air-sensitive solid compound is isolated. It slowly turns dark near the melting point, observed at 60°C in agreement with previous data [14]. A mass spectrum and Cl analysis for 1 were obtained, the results of which are presented below. The vapor pressure of the solid was determined by the transport method, and found to be 1.8×10^{-2} torr at 57°C and 7.1×10^{-3} torr at 50°C .

2.2. OMCVD apparatus

Preliminary experiments were performed in a short path hot wall CVD reactor described in [15]. However

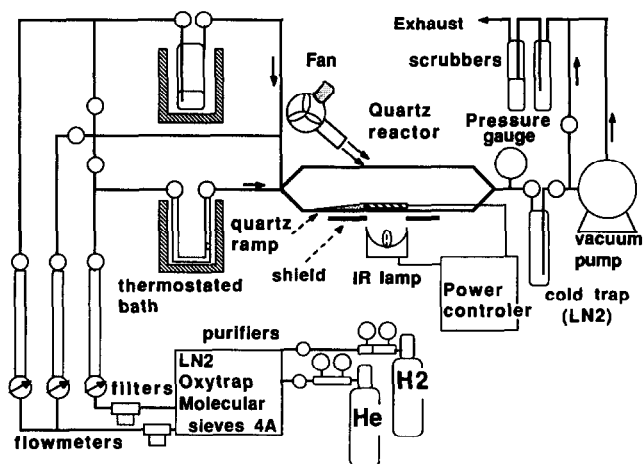


Fig. 1. Schematic diagram of the OMCVD apparatus, reproduced by permission from Ref. 13.

TABLE 1. Typical OMCVD growth conditions used for CoGa thin film deposition using $(\text{CO})_4\text{CoGaCl}_2(\text{THF})$ (1) as a single source precursor

	Reactor type		
	Hot wall	Cold wall	Cold wall
Total pressure (torr)	760	760	0.9–6
Substrate temperature ($^\circ\text{C}$)	500	200–250	250–400
Total flow rate (sccm)	20	600	5–25
Carrier gas	H_2	$\text{He} + \text{H}_2$	$\text{He} + \text{H}_2$
H_2 mole fraction	1	0.25–1	0–1
Precursor bubbler temperature ($^\circ\text{C}$)	–	60–63	50
Typical growth rate (nm/h)	100	38–60	90–1800

for an epitaxial growth, on one hand a sufficiently high substrate temperature is required in order to have a high surface diffusivity of the adsorbed species, and on the other hand, the growth rate of the film should be independent of the surface orientation. Such requirements are satisfied when the process is controlled by the mass-transport through a gas phase boundary layer above the substrates. In an isothermal reactor, it is very difficult to work in a kinetic regime favorable to an epitaxial growth, namely the mass-transport limited regime. This is mainly due to depletion of the precursor because of gas phase reactions. As a consequence, epitaxial growth is usually conducted in non-isothermal reactors. Deposition experiments were performed in a horizontal cold wall laminar flow CVD reactor (Fig. 1) identical to that used for the deposition of III–V semiconductor epilayers [13]. It is equipped with external focussed infrared lamp and has been successfully used for CoGa epitaxial growth using two separate sources. The typical OMCVD growth conditions are summarized in Table 1.

2.3. General instrumentation

The mass spectrum of 1 has been recorded under electronic impact using an ionisation energy = 70 eV (source temperature = 120°C). Thermogravimetric analyses were performed using a Du Pont Analyzer No. 951 with either Ar or H_2 flowing through the furnace. The film morphologies were analyzed by scanning electron microscopy (SEM) and their structure by X-ray diffraction (XRD). The composition of the films deposited on (100)Si and Al_2O_3 , where interference from GaAs is absent, was determined by energy dispersive X-ray analysis (EDX).

3. Screening of the precursor

3.1. Mass spectrometry analysis

This technique is useful to investigate the labile groups and to obtain meaningful information about the

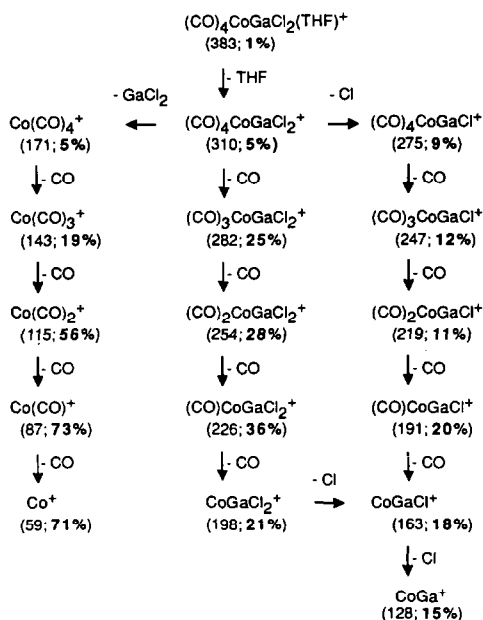


Fig. 2. Principal fragmentation patterns of $(\text{CO})_4\text{CoGaCl}_2(\text{THF})$ (1) under electronic impact. The values reported under each ion are the mass/charge ratio and their relative intensity (%) compared to the main peak THF^+ ($m/e = 72$; 100%). Other peaks observed are given in the text.

decomposition process. The peaks are easily identified from the isotopic ratio of Ga 69 (60%) and 71 (40%) and Cl 35 (76%) and 37 (24%). The principal fragmentation pattern and peak assignments are given in Fig. 2. In addition, we obtained evidence of a partial disproportionation of 1 into $\text{ClGa}[\text{Co}(\text{CO})_4]_2(\text{THF})$, and GaCl_3 , by observation of a high-mass series of peaks arising from the successive loss of CO from $[\text{ClGaCo}_2(\text{CO})_7]^+$ through $[\text{ClGaCo}_2(\text{CO})_2]^+$ at $m/e = 418$ (21%), 390 (10%), 362 (7%), 334 (6%), 306 (11%) and 278 (20%), respectively. No peak is observed above m/e of 442, indicating that the parent ion $[\text{ClGa}(\text{Co}(\text{CO})_4)_2(\text{THF})]^+$, MW = 519.2, is too unstable to be observed. The fact that this disproportionation occurs only upon heating the sample in the mass spectrometer is supported by analysis of the starting material which is found to contain 19.28 at.% Cl [16]; calculated for $\text{CoGaCl}_2\text{C}_8\text{H}_8\text{O}_5$, 18.48 at.%, and for $\text{Co}_2\text{GaClC}_{12}\text{H}_8\text{O}_9$, 6.8 at.%. The parent molecular ion for 1 ($m/e = 383$) is observed at only very low intensity (1%) and the lability of CO groups in this complex is revealed by a series of peaks at $m/e = 383$, 355, 327, 299 and 271 which, however, all have an intensity lower than 2%.

Apart from these two series of peaks, the mass spectrum is fully analyzed from the fragmentation pat-

tern shown in Fig. 2. It is assumed that the THF elimination is the initial step which gives $[(\text{CO})_4\text{CoGaCl}_2]^+$ at $m/e = 310$. Then, the successive elimination of CO groups reveals three different pathways: (i) from this parent entity, (ii) after dissociation of the intermetallic bond and loss of GaCl_2 and (iii) after the release of one Cl. The second pathway gives evidence for the dissociation of the Co–Ga bond since this is the fragmentation of the component $[\text{Co}(\text{CO})_4]^+$. However, the relatively high intensity of the ions observed in the two other pathways argues for a good stability of this intermetallic bond since the release of the ligands continues up to $[\text{CoGa}^+]$ (15%). Although $[\text{GaCl}_2]^+$ and $[\text{GaCl}^+]$ have quite the same intensity ($\sim 10\%$) all the peaks $[(\text{CO})_x\text{CoGaCl}_2]^+$ ($x = 0$ to 4) are higher than $[(\text{CO})_x\text{CoGaCl}^+]$ indicating that the CO loss from $[(\text{CO})_4\text{CoGaCl}_2]^+$ is probably the dominant route. Furthermore, the relatively high intensity and the number of peaks containing at least one Cl atom bonded to Ga confirms the high stability of the Ga–Cl bond (mean bond strength ~ 90 kcal/mol in GaCl_3).

3.2. Thermogravimetric analysis

As shown in Fig. 3, the decomposition process of 1 under Ar atmosphere occurs apparently in a single step in the range ~ 100 to $\sim 230^\circ\text{C}$. There is no obvious correlation between the weight loss and the elimination of an integral number of ligands. The solid residue is about 40% of the starting material that is significantly higher than that calculated for CoGa (33.5 wt.%). By contrast, under a stream of H_2 of varying total flow rate and hydrogen partial pressure, consistent evidence is obtained for a multistep (at least three) decomposition process. The slight difference of slope below 100°C

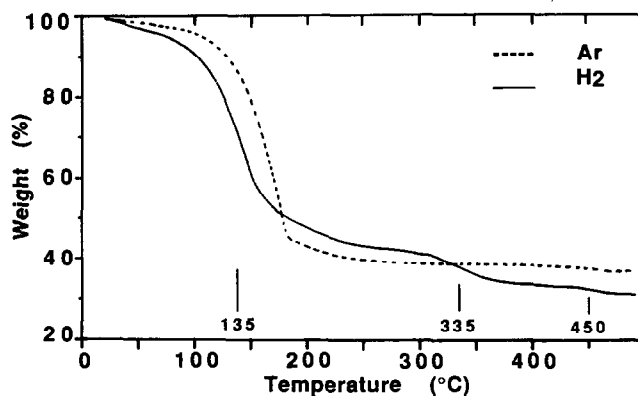


Fig. 3. TGA of $(\text{CO})_4\text{CoGaCl}_2(\text{THF})$ recorded using an inert carrier gas (Ar) on a reducing carrier gas (H_2). The total flow rate is $100\text{ cm}^3/\text{min}$.

is probably due to an earlier onset of decomposition. The first step is the most efficient and occurs $\sim 25^\circ\text{C}$ lower than under Ar atmosphere. At this stage, the solid residue is $\sim 44\%$ by weight. Then, the decomposition continues with the subsequent loss of $\sim 8\text{ wt.}\%$ and $3\text{--}4\text{ wt.}\%$ in a second and third step, respectively. The decomposition is complete above $400\text{--}450^\circ\text{C}$, depending on the total flow rate. The solid residue is $\sim 33\text{ wt.}\%$, close to the value calculated for CoGa. The EDX analysis of this powder has revealed, in spite of its inhomogeneity, a low content of Cl and a Co/Ga intensity ratio close to that of a bulk $\text{Co}_{0.5}\text{Ga}_{0.5}$ sample used as standard. These observations argue roughly for the successive removal of the two Cl atoms during the second and third step respectively (weight loss for Cl $8\text{ wt.}\%$). The decomposition process is then found to be cleaner under H_2 atmosphere and probably different than under inert atmosphere.

4. OMCVD results

4.1. Deposition in an isothermal CVD reactor

Short path vapor transport of **1** under a H_2 stream in a hot wall CVD reactor leads to thin films of CoGa at 500°C . Films are highly reflective, polycrystalline and single phased. A slight contamination by oxygen is detected by Auger analyses but all the Cl from the precursor has been removed in this process [9]. XRD patterns do not reveal any preferential orientation of the films grown on the various substrates used.

4.2. Deposition in a cold wall CVD reactor

Under atmospheric pressure, very thin films are grown on the substrates in the narrow temperature range $200\text{--}250^\circ\text{C}$. This contrasts with experiments performed in the isothermal reactor [9]. From thickness measurements, the growth rate is estimated to be 60 nm/h at 200°C . Increasing the temperature, the growth rate decreases due to depletion of the precursor in the gas phase. Above 250°C , decomposition occurs in the gas phase and a coating is observed only on the reactor wall above the sample. The growth rate, which is low, is in part related to the low evaporation rate of the precursor under atmospheric pressure (typically $3.5 \times 10^{-5}\text{ mol/h}$) due to its low vapor pressure.

A decrease of the total pressure to 6 torr increases the evaporation rate of the precursor by a factor 3 to 5, depending on the flow rate of the carrier gas through the bubbler. Furthermore, gas phase decomposition is drastically reduced due to a decrease of the dwelling time of the species in the reaction zone. As a result, the deposition of intermetallic films on the various substrates is obtained up to 400°C . The films have a metallic brightness and SEM observations reveal a

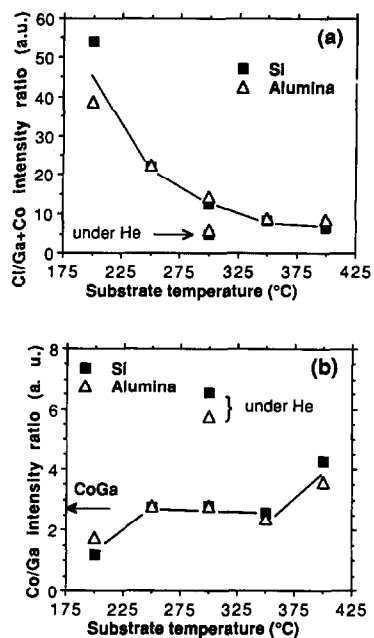


Fig. 4. Variation of the composition of films deposited on (100)Si and Al_2O_3 as a function of the substrate temperature: (a) EDX $\text{K}\alpha$ intensity ratio $\text{Cl}/\text{Co} + \text{Ga}$; (b) EDX $\text{K}\alpha$ intensity ratio Co/Ga . The arrow in (b) indicates the value of the Co/Ga ratio for a $\text{Co}_{0.5}\text{Ga}_{0.5}$ standard. A partial pressure of H_2 has been used in all experiments except one, noted in the figure, which was carried out under He at 300°C .

glossy surface for the films grown on (100)GaAs. Their growth rate is significantly higher than under atmospheric pressure.

As shown in Fig. 4(a), EDX analyses reveal that Cl is incorporated in the films but this contamination decreases when the deposition temperature increases. The ratio $\text{Co}/\text{Ga} = 1$ imposed by the single source precursor is maintained in the films grown between $250\text{--}350^\circ\text{C}$. Below this temperature range, the lower value of the $\text{K}\alpha$ intensity ratio Co/Ga associated with the high Cl contamination argues for the presence of gallium chlorides in the films. Above 350°C the films are found to be Co-rich (Fig. 4(b)). The CoGa films deposited under inert atmosphere (without H_2) contain an excess of Co accompanied by only a slight Cl contamination. Thus in absence of H_2 , Cl elimination is coupled with loss of Ga.

As revealed by XRD, all the samples prepared in the cold wall reactor have a poor crystallinity. The patterns are characteristic of an amorphous structure. They exhibit only a broad peak centered at $2\theta = 44^\circ$ assigned to the (110) reflection of the cubic phase $\beta\text{-CoGa}$ (Fig. 5(a)). This reflection has the highest structure factor (intensity) of the overall reflections of this phase, as observed with the polycrystalline films

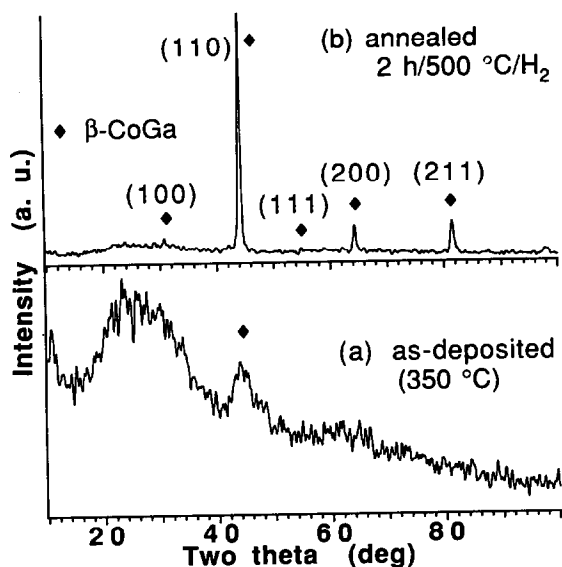


Fig. 5. XRD patterns of CoGa thin films deposited on amorphous silica: (a) As-deposited microcrystalline film (350°C); the broad peak between $2\theta = 20$ to 34° is due to the substrate; (b) After annealing 2 h at 500°C under hydrogen atmosphere.

deposited at 500°C in the isothermal reactor [15]. According to the Scherrer's formula [17], the mean crystallite dimensions perpendicular to the (110) planes are calculated to be in the range 15–25 Å, depending on the deposition temperature. After annealing for 2 h at 500°C under hydrogen atmosphere, the single phased β -CoGa structure is clearly obtained without any preferential orientation either on silica or on (100)GaAs (Fig. 5(b)).

5. Discussion

5.1. Influence of the temperature

The different results obtained in the isothermal and the cold wall CVD reactors can be mainly explained by

the change of the deposition temperature. Both the lower purity and crystallinity of the films grown in the cold wall reactor originate from the lower deposition temperature. The decrease of Cl contamination by increasing the temperature is in agreement with the results obtained in isothermal reactor (no Cl incorporation at 500°C) and also with TGA analyses, which have shown that a complete elimination of Cl is expected only above 450°C. This is also related to the relatively high volatility of gallium chlorides (GaCl₃: b.p. 201°C; Ga₂Cl₄: b.p. 535°C). In the temperature range 250–350°C, the film stoichiometry is fixed at Co/Ga = 1, like in the starting precursor, as long as the intermetallic Co–Ga bond is not dissociated. This agrees fairly well with the mass spectroscopic analysis which has revealed the good stability of this bond. However, its dissociation occurs probably above 350°C. In such conditions, gallium chlorides are removed from the deposition zone because of their high thermal stability and volatility, resulting in the deposition of Co-rich CoGa films. Similar observations have been made using adducts for the deposition of III–V semiconductor compounds [3]. Hydrogen is required cleanly to remove Cl, probably in the form of HCl. Under inert atmosphere, this mechanism cannot occur resulting again in a dissociation of the intermetallic Co–Ga bond, elimination of gallium chlorides and deposition of Co-rich films.

5.2. Influence of the pressure

There are several advantages in decreasing the total pressure in a CVD reactor, specially using single source precursors. Generally, such organometallic compounds have a bulky molecular structure and a low vapor pressure, as is the case with 1. To compensate for this, the reduced pressure increases the evaporation rate and its diffusion coefficient in the gas phase ($D \propto P^{-1}$). Furthermore change of pressure affects the hydrodynamics of the reactor. We demonstrate here that re-

TABLE 2. Flow characteristics in the CVD reactor for typical depositions conditions

Run	T (°C)	P (torr)	Flow (sccm)	Re ^a	Gr ^b	Gr/Re ²	Comment
1 ^c	500	760	20	0.11	~ 0	~ 0	poly-CoGa film
2 ^d	200	760	600	1.30	1814	1073	very thin film
3 ^d	300	760	600	1.03	1532	1444	no film; deposit on top wall
4 ^d	300	6	25	0.09	0.18	22	CoGa(Cl) film
5 ^d	400	6	25	0.09	0.14	17	CoGa(Cl, C) film

^a $Re = (DV\rho)/\mu$, where D = diameter of the tube, V = mean flow velocity, ρ = density of the gas and μ its dynamic viscosity. ^b $Gr = (\alpha g \rho^2 D^3 \Delta t)/\mu^2$, where α = coefficient of thermal expansion, g = gravitational acceleration, $\Delta T = T_{\text{bottom}} - T_{\text{top}}$ and the other parameters have the same meaning as in (a). ^c Isothermal CVD reactor. ^d Cold wall CVD reactor.

duction of pressure has made possible to increase the deposition temperature and consequently, to improve the quality of the CoGa films.

The flow through an isothermal, constant diameter tube reactor due to an imposed pressure gradient is called forced convection. It is characterized by its Reynolds number (Re) [18,19] (Table 2). As a first approximation, Re is independent of the pressure, P , because the density of the gas, ρ , is proportional to P while the mean flow velocity, V , is proportional to P^{-1} . In a non-isothermal CVD reactor a vertical flow due to buoyancy forces and natural (free) convection occurs because of a temperature gradient above the substrate (cold wall). In heat transfer theory, such flow is characterized by its Grashof number (Gr) (Table 2). Here, in first approximation, Gr depends strongly on the pressure because $Gr \propto \rho^2$. The values of Re and Gr as well as the Gr/Re^2 ratio (which characterizes the competition between forced and free convection) are reported in Table 2 for typical deposition experiments. The calculation parameters were taken from Giling [20].

It can be seen that for all the conditions a laminar flow without rippling ($Re < 25$) is expected using H_2 as carrier gas. Both the high values of Gr and the Gr/Re^2 ratio ($Gr/Re^2 \gg 16$) indicate that the flow tends to be dominated by free convection for experiments performed under atmospheric pressure. By contrast, under low pressure the forced flow tends to be dominant. Under atmospheric pressure, an increase of the temperature from 200 to 300°C increases the contribution of the natural convection (Gr/Re^2 increase); this leads to gas phase decomposition of the precursor and deposition on the reactor wall rather than on the substrate, as observed. This effect precludes to increase the substrate temperature beyond 250°C, far from the value of 400°C predicted for a cleaner decomposition, both by TGA analyses and experiments in the isothermal reactor. For this goal, a reduced pressure is beneficial and a thin film can be grown easily up to 400°C. Unfortunately, due to temperature the films are darker, possibly because of a carbon contamination. Furthermore, they become Co-rich probably because of the dissociation of the intermetallic Co–Ga bond in the gas phase.

6. Conclusions

In this work we confirm that the typical drawback of lower vapor pressure for a single source precursor can be overcome by reducing pressure in the CVD reactor. Some features in the design of a single source precursor are contradictory. In the particular case where there is a direct chemical bond between the metal atoms, as in **1**, the ligands should be removable before

dissociation of the intermetallic bond. However, when heteroatoms like Cl are used to stabilize the molecule, their bonds to the metals may be stronger than the intermetallic bond. In a dichloro complex such as **1**, we have shown that removal of one of the Cl atoms occurs relatively easily under hydrogen atmosphere but elimination of the second Cl atom is more difficult. As a consequence, at moderate temperatures the CoGa films are slightly contaminated by Cl. Furthermore, the adsorbed species resulting from **1** probably has a low surface diffusion due to its molecular bulk. This precludes an epitaxial growth and favors a disordered, amorphous product as observed. The present single source precursor is not suitable for deposition of Ga-rich (64 at.% Ga) β -CoGa which is required for lattice matching to (100)GaAs. However, the stoichiometric control achieved in the present work indicates that single source precursors containing the ratio $CoGa_2$ could be of use in such work.

Acknowledgments

We thank Dr. Richard Lysee and A.A. Talin for assistance in the XRD analyses and Dr. Dilip Sen-sharma for EIMS measurements. Dr. F. Maury was supported by a grant from the CNRS (Centre National de la Recherche Scientifique) in cooperation with NSF (National Science Foundation). Dr. L. Brandt was supported by a grant from the DFG (Deutsche Forschungsgemeinschaft).

References

- 1 R. A. Jones, A. H. Cowley and J. G. Ekerdt, *Mater. Res. Soc. Symp. Proc.*, 204 (1991) 73.
- 2 A. H. Cowley and R. A. Jones, *Angew. Chem., Int. Ed. Engl.*, 28 (1989) 1208.
- 3 F. Maury, *Adv. Mater.*, 3 (1991) 542.
- 4 D. V. Baxter, M. H. Chisholm, V. F. DiStasi and J. A. Klang, *Chem. Mater.*, 3 (1991) 221.
- 5 C.-S. Jun, T. P. Fehner and G. J. Long, *Chem. Mater.*, 4 (1992) 440.
- 6 B. J. Aylett, in R. M. Laine (ed.), *Transformation of Organometallics into Common and Exotic Materials: Design and Activation*, NATO Ser., Ser. E, Martinus Nijhoff Publishers, Vol. 141, 1988, p. 165.
- 7 M. E. Gross and J. Lewis, *J. Vac. Sci. Technol. B*, 6 (1988) 1553.
- 8 C. L. Czekaj and G. L. Geoffroy, *Inorg. Chem.*, 27 (1988) 8.
- 9 Y. J. Chen, H. D. Kaesz, Y. K. Kim, H.-J. Müller, R. S. Williams and Z. Xue, *Appl. Phys. Lett.*, 55 (1989) 2760.
- 10 (a) R. A. Fischer, H. D. Kaesz, unpublished observations; (b) R. A. Fischer, H. D. Kaesz, S. I. Khan and H.-J. Müller, *Inorg. Chem.*, 29 (1990) 1601; (c) T. B. Massalski (ed.), *Binary Alloys Phase Diagrams*, 2nd Ed., ASM International, Vol. 2, 1990, 1840.
- 11 D. A. Baugh, A. A. Talin, R. S. Williams, T.-C. Kuo and K. L. Wang, *J. Vac. Sci. Technol. B*, 9 (1991) 2154.
- 12 F. Maury, A. A. Talin, H. D. Kaesz and R. S. Williams, *Appl. Phys. Lett.*, 61 (1992) 1075.

- 13 F. Maury, A. A. Talin, H. D. Kaesz and R. S. Williams, *Chem. Mater.*, 5 (1993) 84.
- 14 D. J. Patmore and W. A. G. Graham, *Inorg. Chem.*, 5 (1966) 1586.
- 15 H. D. Kaesz, R. S. Williams, R. F. Hicks, J. I. Zink, Y. J. Chen, H. J. Müller, Z. Xue, D. Xu, D. K. Shuh and Y. K. Kim, *New J. Chem.*, 14 (1990) 527.
- 16 Elemental analysis of Cl was performed by Galbraith Laboratories, Inc., Knoxville, TN.
- 17 H. P. Klug and L. E. Alexander, *X-ray Diffraction Procedures for Polycrystalline and Amorphous Materials*, J. Wiley & Sons, New York, 1954.
- 18 R. B. Bird, W. E. Stewart and E. N. Lightfoot, *Transport Phenomena*, J. Wiley & Sons, New York, 1960.
- 19 H. Schlichting, *Boundary-layer Theory*, 6th Ed., McGraw-Hill, New York, 1968.
- 20 L. J. Giling, *J. Electrochem. Soc.*, 129 (1982) 634.